

A Novel 3D Finite Element Simulation Model for the Prediction of the Residual Stress State after Shot Peening

M. Zimmermann 1, V. Schulze 1, H. U. Baron 2, D. Löhe 1

1 Institute for Materials Science and Engineering I, University of Karlsruhe

2 MTU Aero Engines, Munich

ABSTRACT

3D Finite-Element shot peening models known from literature do not take into account component thickness as a geometric parameter influencing the residual stress state after shot peening. Hence classic approaches and a new approach of model constraints were investigated for their capability to contribute to a realistic prediction of the residual stress state after a shot peening treatment. The numerical results obtained were compared with x-ray measurements. The strain rate dependent deformation behavior of the investigated and aged material IN718 was taken into account using an elasto-viscoplastic material model with combined isotropic and kinematic hardening. It was found that a small thickness has no influence on the compressive residual stresses in the surface region but great influence on the tensile residual stresses present in deeper regions. The new approach of model constraint takes into account deflection effects and yields to a very good accordance with experimental results.

KEY WORDS

Shot Peening, simulation, material modeling, IN718, curved surfaces

INTRODUCTION

Compressive residual stresses are induced during shot peening in the surface near regions of a treated component and are balanced by an almost constant tensile residual stress field in greater depths (Menig, 2000). For bulky components the tensile stresses are small because of the available thickness on which the compressive stresses are balanced. However since shot peening is also applied on rather thin components such as turbine blades, it can be assumed that larger tensile residual stresses can be found in the inner component regions representing a potential risk to crack initiation during service. Hence thickness has to be taken into account as a geometric parameter influencing the residual stress state of a component. Since tensile residual stresses are located in the deeper regions of a component their experimental determination by x-ray or neutron measurement is quite costly. Hence FE simulation of shot peening is an interesting approach of analyzing component thickness as a geometric parameter. On this account the motivation of this work arises to find a suitable type of boundary condition, which is capable to realistically describe the influence of component thickness on the residual stress state.

METHODS

Experimental Procedure

In order to analyze the geometry parameter thickness on the residual stress state experimentally and to provide experimental data for the comparison with the simulation model a test specimen featuring three sections of different thickness (cp. Figure 1) was

treated with an air blast machine (type Baiker) with the following peening parameters: mass flow 5 kg/min, impact angle 80° , shot media CCW31 with a measured mean diameter of 0.89 mm, air pressure 1bar, coverage 98 %. The mean shot velocity was determined by means of an optical measuring system provided from KSA (Wüstefeld, 2005) to 23 m/s. The impact angle is defined according to Figure 1. The material of the test specimen was age hardened IN718. The residual stresses after shot peening were measured by x-ray diffraction on the $\{311\}$ -interference line using Mn- $K\alpha$ -radiation. The measured interference peaks were evaluated according to the $\sin^2\psi$ method, using a Young's modulus of $E^{311} = 200000$ MPa and a Poisson's ratio of $\nu^{311} = 0.32$. Measurements in depth were performed by previous electro polishing. Stress relaxation due to the material removal by electro polishing was not taken into account, since the removed area was small. The test specimens were separated after the shot peening treatments at the positions shown in Figure 1 in order to enable the x-ray diffraction measurement in the x-direction at the test specimen sections with a thickness of 5 and 1 mm. After the treatments the test specimen section with a thickness of 1 mm was slightly bent around the y-axis and after the separation also around the x-axis.

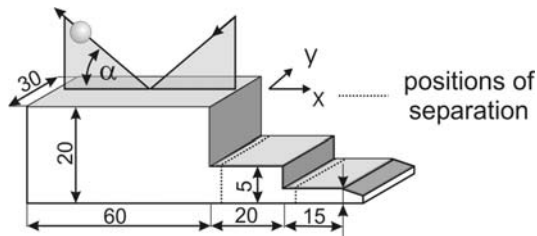


Figure 1 : Test specimen geometry, coordinate system and positions of separation.

Figure 1 : Test specimen geometry, coordinate system and positions of separation. The residual stresses after shot peening were measured by x-ray diffraction on the $\{311\}$ -interference line using Mn- $K\alpha$ -radiation. The measured interference peaks were evaluated according to the $\sin^2\psi$ method, using a Young's modulus of $E^{311} = 200000$ MPa and a Poisson's ratio of $\nu^{311} = 0.32$. Measurements in depth were performed by previous electro polishing. Stress relaxation due to the material removal by electro polishing was not taken into account, since the removed area was small. The test specimens were separated after the shot peening treatments at the positions shown in Figure 1 in order to enable the x-ray diffraction measurement in the x-direction at the test specimen sections with a thickness of 5 and 1 mm. After the treatments the test specimen section with a thickness of 1 mm was slightly bent around the y-axis and after the separation also around the x-axis.

Shot Peening Model

The shot peening model consists of a 3-dimensional rectangular body of arbitrary thickness and quadratic base and is based on the work of (Schwarzer, 2003). ABAQUS/Explicit is used for the dynamic analysis of the shot impacts on the surface taking into account inertia effects. The mesh is set up by 8-node linear brick elements with reduced integration and hourglass control. The element size of a surface element was adjusted to 1/15th of the dimple diameter produced by a single shot impact for the given shot diameter and velocity. The problem of damping of induced and internally reflecting stress waves in the model is solved using so-called infinite elements surrounding the faces of the rectangular body. These special types of elements lead to a minimization of the reflection of dilatational and shear waves into the body during the analysis and do not affect the stress state of the model when static equilibrium is reached (ABAQUS manuals, 2007). The steel shots are modeled by half spherical rigid surfaces with parameterized diameter, velocity, and direction. The

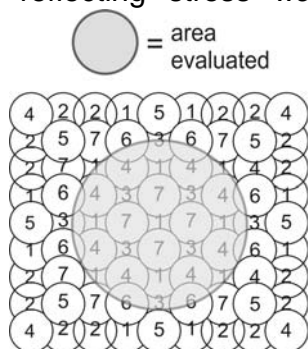


Figure 2 : Shot arrangement and evaluated area to calculate the residual stress profile; numbers indicate the impact order of the shots.

mechanical properties of a full sphere are provided to the rigid surfaces by connecting each one of them to a point mass and a rotary inertia element located in the center of the spheres. Isotropic Coulomb friction between the shots and the surface of the plates is assumed with a constant friction coefficient $\mu = 0.4$. The stochastic impact order of the shots on the treated surface is modeled by a dimple pattern of full coverage of the entire model surface with the impact order and shot arrangement shown in

Figure 2 providing an axis-symmetric residual stress state in the case of an impact angle $\alpha = 90^\circ$. The residual stresses from the simulation are determined according to

(Schwarzer, 2003) with an averaging technique where the residual stresses of the elements lying within the gray marked circular are averaged for every depth layer.

Boundary Conditions

Three types of boundary conditions were investigated in this study. The first type corresponds to the boundary condition used by (Schwarzer, 2003) where the lateral faces of the model are not constrained and the model's base is fixed in z-direction (cp. Figure 3 a). The second type is the classic approach applying symmetric boundary conditions to the lateral faces and the third and new type of boundary condition aims to model a small section of an initially flat plate with a defined thickness where deflection can occur depending on the thickness and the peening intensity. The lateral faces of the model are forced to be perpendicular to the surface as well to the base by a kinematic coupling constraint of the lateral faces in normal direction with 4 reference points surrounding the model according to Figure 3 b). Control of deflection is established by constraining the rotational degree of freedom of the reference points. This is important when deflection is omitted due to geometrical constraints like for instance the deflection of the 1mm thick section of the test specimens around the x axis during the shot peening treatment.

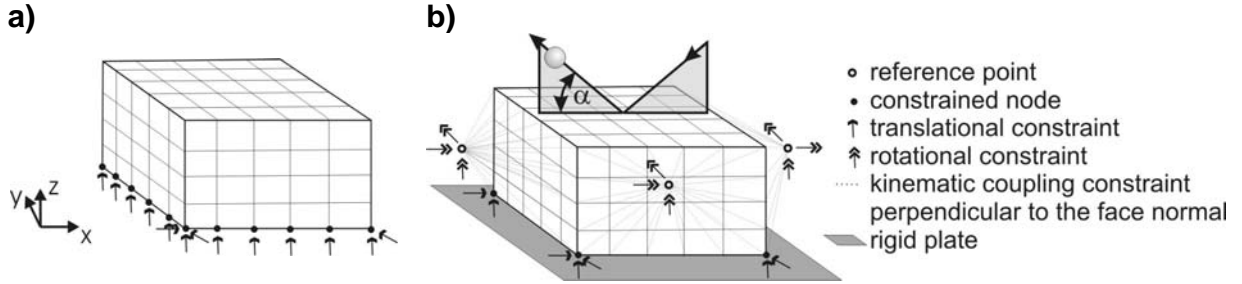


Figure 3: Boundary conditions with a) free and b) constraint lateral faces.

Material Model

To take into account the Bauschinger effect and strain rate sensitivity of aged IN718 a combined isotropic/kinematic elastoviscoplastic material model is used for the shot peening simulation and was implemented into ABAQUS/Explicit as a user defined subroutine. This material model is an extended version of the unified constitutive material model proposed by (Ramaswamy, 1990) and consists of a set of ordinary partial differential equations, which are presented in rate form:

$$\dot{\varepsilon} = \dot{\varepsilon}^E + \dot{\varepsilon}^I \quad (1)$$

$$\dot{\varepsilon}_{ij}^I = D_0 \exp \left[-\frac{1}{2} \left(\frac{Z^2}{3K_2} \right)^n \right] \frac{S_{ij} - \Omega_{ij}}{\sqrt{K_2}} \quad (2)$$

$$\dot{\Omega}_{ij} = \dot{\Omega}_{1,ij} + \dot{\Omega}_{2,ij}, \quad \dot{\Omega}_{1,ij} = \frac{2}{3} a_1 \dot{\varepsilon}_{ij}^I - a_1 \frac{\Omega_{1,ij}}{\Omega_{1,m}} \dot{\varepsilon}_e^I, \quad \dot{\Omega}_{2,ij} = \frac{2}{3} a_2 \dot{\varepsilon}_{ij}^I - a_2 \frac{\Omega_{2,ij}}{\Omega_{2,m}} \dot{\varepsilon}_e^I \quad (3, 4, 5)$$

$$\dot{Z} = m(Z_1 - Z) \dot{\varepsilon}_e^I \quad (6)$$

$$\text{with } K_2 = \frac{1}{2} (S_{ij} - \Omega_{ij})(S_{ij} - \Omega_{ij}) \text{ and } \dot{\varepsilon}_e^I = \sqrt{\frac{2}{3} \dot{\varepsilon}_{ij} \dot{\varepsilon}_{ij}}$$

Equation (1) is the general kinematic equation combining elastic ε^E and inelastic strain ε^I to total strain ε . The inelastic strain rate $\dot{\varepsilon}^I$ is calculated by the flow equation (2) as a

function of deviatoric stress S and two state variables, namely the back stress Ω and the scalar drag stress Z . Strain rate sensitivity is governed by the model parameters D_0 , correlating with the maximum plastic strain rate of the material, and n . The extension of the material model from (Ramaswamy, 1990) consists in a decomposition of the back stress Ω into two back stress terms Ω_1 and Ω_2 , which develop according to equation (4) and (5) during plastic deformation. This decomposition yields to a better description of the cyclic deformation behaviour of the material (Lemaitre, 1999) by means of the material model parameters a_1 , a_2 , $\Omega_{1,m}$, and $\Omega_{2,m}$. Equation (6) is the evolution equation of the drag stress Z . m and Z_1 are material model parameters and $\dot{\epsilon}_e^I$ is the effective plastic strain rate. The procedure to determine the material model parameters is divided into two steps. In the first step the parameters n governing the strain rate sensitivity and the initial flow stress of the material represented by the parameter $Z_0 = Z(\dot{\epsilon}_e^I = 0)$ were determined on the basis of compression tests carried out at strain rate regimes ranging from 10^{-3} to 10^{+4} 1/s with the method of least squares. D_0 was set to 10^6 1/s. The remaining material model parameters (a_1 , a_2 , $\Omega_{1,m}$, $\Omega_{2,m}$, m and Z_1) describe the deformation and hardening behaviour and are fitted in a second step of the material model parameter determination procedure by means of the commercial software (FitIt) on basis of strain controlled push pull tests, which provide information about the deformation behaviour during cyclic loading conditions.

RESULTS AND DISCUSSION

A comparison with experimental data validates the capability of the material model to account for strain rate sensitivity for all measurable strain rate regimes and for the Bauschinger effect during cyclic loading conditions (Zimmermann, 2008). Consequently a material model is provided to the shot peening simulation that should meet the requirements for realistically describing the material behavior of a component during shot peening.

In order to investigate the capability of the three types of boundary conditions to realistically constrain the simulated body for different thicknesses simulations with the 3 types of boundary conditions were carried out with a model thickness of 1 and 5 mm. The calculated residual stress depth profiles are compared to the experimental measurements in Figure 4. The symmetric boundary conditions yield to a good prediction of the compressive residual stresses close to the surface. However the calculated residual stress depth profile is unbalanced since no tensile residual stresses are present. This shortcoming is due to external nodal forces on the lateral faces representing the infinite lateral extension. Hence the calculated stress state with symmetry boundary conditions on the lateral faces is not internally equilibrated and therefore unrealistic if small thicknesses are investigated. In the case of leaving the lateral faces unconstrained qualitatively good accordance to the experimental results is achieved for a thickness of 1 mm. However a thickness of 5 mm the compressive residual stresses in the surface region are strongly under- and the tensile residual stresses strongly overestimated. This effect is due to the smaller stiffness in the edge near regions of the models surface leading to an "out squeezing" which is shown in Figure 5. Overcoming these disadvantages the kinematic coupling constraint suppresses the "squeeze out" effect and enforces the induced compressive residual stresses to be balanced with tensile residual stresses.

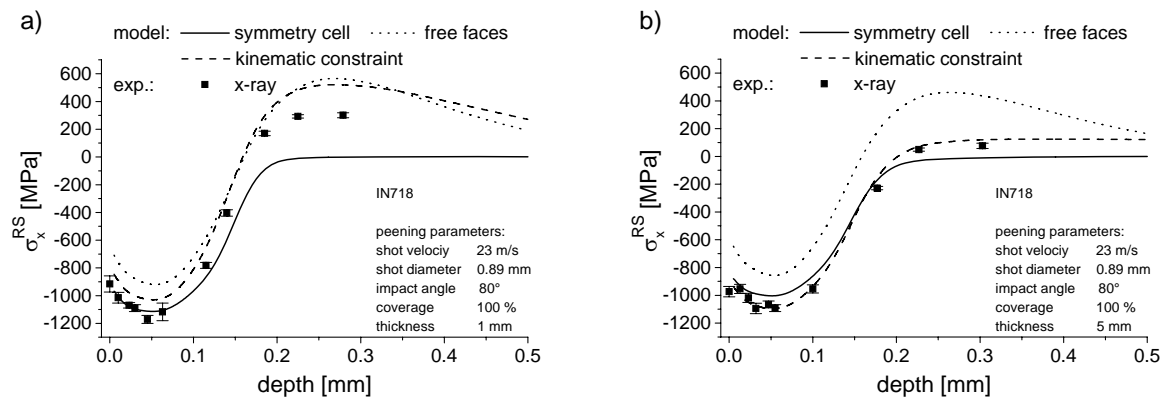


Figure 4: Influence of boundary conditions on the calculated residual stress depth profiles for a thickness of a) 1 and b) 5 mm.

In Figure 6 the capability of the new type of boundary condition describing the influence of thickness on the residual stress state after shot peening is shown. The simulations of a thickness of 5 and 1 mm were carried out suppressing the deflection of the rectangular body around the y axis during the shot impacts, which should represent the geometrical stiffness of the test specimen. The separation of the 5 and 1 mm thick test specimen sections and the corresponding stress relaxation is taken into account by releasing the rotational constraint of the reference nodes linked to the lateral faces normal to the y direction after the shot impacts. The results show that in x-direction no influence of the thickness on the surface and maximum compressive residual stresses can be observed. However, in y-direction the surface and maximum compressive residual stresses for a thickness of 1 mm are smaller. This effect can be attributed to the stress relaxation due to the separation of the test specimen. In both directions increasing tensile residual stresses can be observed with decreasing thickness. The predicted tensile residual stresses for a thickness of 1mm are overestimated in comparison to the x-ray measurements. However, strong stress rearrangement effects due to electro polishing of such a thin test specimen are likely to decrease the measured tensile residual stresses and to be the reason of this deviation.

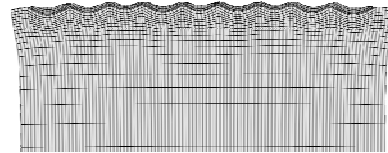


Figure 5: Scaled mesh deformations with free faces (cut view).

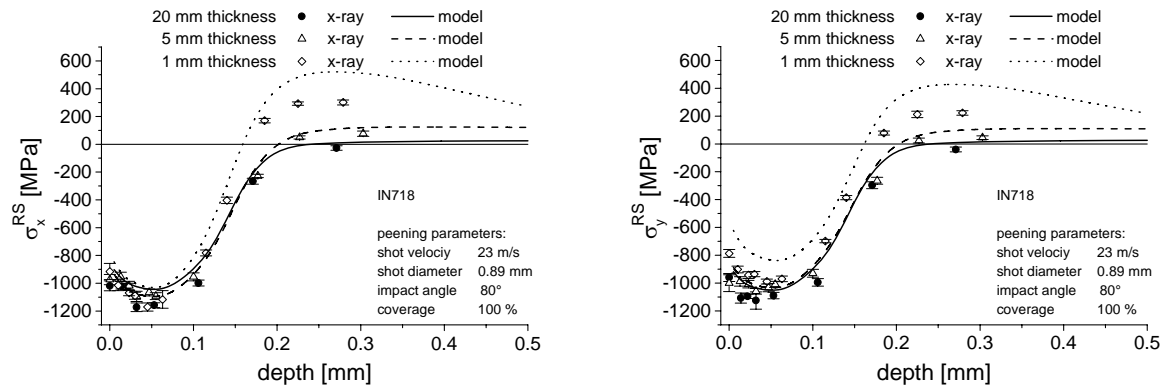


Figure 6: Measured and simulated residual stress depth profiles for different thicknesses.

CONCLUSIONS

The influence of component thickness on the residual stress state after shot peening was analyzed experimentally by x-ray diffraction measurements at a shot peened test specimen featuring different thicknesses and numerically by 3D FE simulations using three different approaches for constraining the model boundaries. It was found that with the classic approach of symmetric boundaries at the lateral model faces the influence of thickness is completely neglected and the residual stress depth profile is not balanced. Leaving the lateral faces free leads to squeezing effects at the edges of the model surface and to unrealistic stress states. Constraining the lateral faces to be perpendicular to the surface as well to the base of the model leads to the incorporation of deflection effects and to realistic simulation results being in very good accordance to the experimental results. The analysis of the influence of thickness on the residual stress state showed that decreasing thickness doesn't affect the compressive residual stresses in the surface region but leads to a shift of the zero crossing to the surface and to higher tensile residual stresses in greater depths. On basis of this observation it can be concluded that the residual stress distribution can be different even when the induced plastic deformations are identical. This means that the residual stress distribution not only depends on the plastic deformation field but also on the geometrical constraints.

ACKNOWLEDGMENTS

The simulations were performed on the national super computer HP XC4000 at the Scientific Supercomputing Center Karlsruhe under the grant number FESSPP. The authors gratefully acknowledge the financial support from the European 6th Framework Programme through the research project VERDI (Virtual Engineering for Robust manufacturing with Design Integration; <http://www.verdi-fp6.org>).

REFERENCES

- ABAQUS Analysis Users Manuals (2007)**, Infinite elements, Section 22.2.1.
- FitIt**, www.fitit.fraunhofer.de
- Lemaitre, J. & Chaboche, J. (1990)**, *Mechanics of solid materials*, Cambridge University Press, 1st edition, pages 233-234.
- Meguid, S. A.; Shagal, G. & Stranart, J. C. (2007)**, 'Development and Validation of Novel FE Models for 3D Analysis of Peening of Strain-Rate Sensitive Materials', *Journal of Engineering Materials and Technology* 129(2), 271-283.
- Menig, R.; Pintschovius, L.; Schulze, V. & Vöhringer, O. (2001)**, 'Depth profiles of macro residual stresses in thin shot peened steel plates determined by X-ray and neutron diffraction', *Scripta Materialia* 45, 977-983.
- Ramaswamy, V. G.; Stouffer, D. C. & Laflen, J. H. (1990)**, 'A Unified Constitutive Model for the Inelastic Uniaxial Response of René 80 at Temperature Between 538 °C and 982 °C', *Journal of Engineering Materials and Technology* 112, 280-286.
- Schulze, V.; Zimmermann, M. & Klemenz, M. (2008)**, State of the Art in Shot Peening Simulation, in 'Proceedings of the Tenth International Conference on Shot Peening'.
- Schwarzer, J.; Schulze, V. & Vöhringer, O. (2003)**, 'Evaluation of the Influence of Shot Peening Parameters on Residual Stress Profiles using Finite Element Simulation', *Materials Science Forum* 462-432, 3951-3956.
- Wüstefeld, F.; Linnemann, W.; Kittel, S. et al. (2005)**, On-Line Process Control for Shot Peening Applications, in 'Proceedings of the Ninth International Conference on Shot Peening'.
- Zimmermann, M.; Schulze, V.; Baron H. U.; Löhe, D. (2008)**, 'Different Approaches Modelling Coverage in 3D Finite Element Simulation of Shot Peening', *Materials Science and Engineering A*, to be submitted.